

# Scaling Properties of the Measure of Constant Topological Entropy

Yuzhen Ge<sup>1</sup>

*Received May 11, 1990; final August 3, 1990*

---

The topological entropy for some families of one-dimensional unimodal maps is studied. By arranging the windows of constant topological entropy in a binary tree, we have obtained the total measure of these windows. The scaling properties of this measure are studied.

---

**KEY WORDS:** Nonlinear dynamics; chaos; one-dimensional unimodal maps; measure; scaling; topological entropy.

## 1. INTRODUCTION

The topological entropy for a dynamical system is defined as

$$h = \lim_{n \rightarrow \infty} \frac{\log N_n}{n} \quad (1)$$

where  $N_n$  is the total number of periodic points in cycles of period  $n$ .

By the definition of the topological entropy, for a one-dimensional quadratic map [the following results can also be applied to other families of unimodal maps, such as map (5)<sup>(1)</sup> although rigorous proof is lacking]

$$x_{n+1} = f_\lambda(x_n) \quad (2)$$

the topological entropy is not zero only in the chaotic regime. As  $\lambda$  increases and before it reaches the first period-doubling bifurcation accumulation point  $\lambda_\infty$ , the topological entropy is zero since there are only finitely many stable and unstable periodic cycles. As  $\lambda > \lambda_\infty$ , all the previous periodic cycles will be unstable and there are infinitely many of

---

<sup>1</sup> Center for Transport Theory and Mathematical Physics, Virginia Tech, Blacksburg, Virginia 24061.

them. Hence the topological entropy is not zero. Since the number of unstable cycles will increase as  $\lambda$  increases, the topological entropy is expected to be an increasing function of  $\lambda$ . As we know, there are infinitely many periodic windows in the chaotic regime. For a parameter in any of these windows there exists a stable periodic cycle (more conditions must be imposed to guarantee uniqueness of the stable periodic cycle). The topological entropy is constant in these windows. Therefore the topological entropy is an increasing function with infinitely many constant steps. Intuitively, the larger the topological entropy, the more chaotic the system is.

We can arrange all the periodic windows in the chaotic regime in a symbolic binary tree.<sup>(1,2)</sup> We will define a window in the parameter axis with constant topological entropy a T-window. Since in a periodic window the topological entropy is constant, a T-window contains one periodic window. The left endpoint of a T-window is the same as that of the periodic window it contains, while the right endpoint is different.

There are different approaches to computing the topological entropy. One intuitive and time-consuming way is to use the definition directly. Biham and Wenzel<sup>(3)</sup> introduced a method to derive all the untangle cycles. We could also use the cycle expansion<sup>(4,5)</sup> approach to compute the topological entropy. But the symbolic alphabet must be obtained to use this method.

We will study two quadratic maps in this paper:

$$x_{n+1} = a - x_n^2 \quad (3)$$

$$x_{n+1} = r(1 - x_n^2) \quad (4)$$

All the quadratic maps are topologically conjugate, i.e., there exists a linear transformation that map (3) can be transformed to map (4) with a rescale of the parameter. It is expected that the topological properties or the metric properties are the same, but some quantities, for example, the sizes of windows, are different.

We will also study a map with quadratic maximum

$$x_{n+1} = r \sin(\pi x_n) \quad (5)$$

and the piecewise linear unimodal map obtained by slicing off all  $x \geq x_p$  of the tent map,

$$\begin{aligned} f_0(x) &= 2x, & 0 \leq x \leq x_p/2 \\ f_c(x) &= x_p, & x_p/2 < x < 1 - x_p/2 \\ f_1(x) &= 2(1 - x), & 1 - x_p/2 \leq x \leq 1 \end{aligned} \quad (6)$$

where  $x_p$  is the parameter of map (6).

In the next section, we will construct the windows of constant topological entropy. In Section 3 the measure of these windows and their scaling properties will be studied.

## 2. WINDOWS OF CONSTANT TOPOLOGICAL ENTROPY

The symbolic dynamics is defined as in refs. 1 and 6, i.e., for a point  $x$ , if  $f^k(x) > c$ , then  $I_k = R$ ; if  $f^k(x) < c$ , then  $I_k = L$ ; else  $I_k = c$ , where  $c$  is the critical point of the unimodal map.  $I_0 I_1 I_2 \dots$  is the itinerary or symbolic sequence. In the following, 1 and 0 may be used interchangeably as  $R$  and  $L$ , respectively. If  $P$ , a symbolic sequence composed of  $R$  and  $L$ , contains an even number of  $R$ 's, we say  $P$  is even; otherwise,  $P$  is odd. A superstable cycle is the one with  $c$  as a point in the orbit. A superstable symbolic sequence is a symbolic sequence starting from  $c$  and ending with  $c$  and thus corresponding to a superstable cycle. In the following, we will always start from  $c$  to construct the symbolic dynamics and  $c$  will be ignored.

As in refs. 2 and 6, the periodic windows in the chaotic regime can be arranged in a binary tree. Each of these windows is represented by a superstable symbolic sequence. Similarly, we can arrange all the T-windows in the same symbolic binary tree with each T-window being represented by the same corresponding superstable symbolic sequence. The left endpoints of the windows are the same as those of the periodic windows, while the right endpoints are different.

Considering the T-window denoted by the superstable orbit  $RL$  or  $10$ , for a parameter value in the neighborhood of the superstable parameter value, the symbolic sequence is either  $\overline{RLR}$  or  $\overline{RLL}$ . We know  $RLR < RLL$ , or  $\lambda_{\overline{RLR}} < \lambda_{\overline{RLL}}$  ( $\bar{P}$  is defined as  $PPPPP\dots$ ).<sup>(2,6)</sup> For maps (3)–(5) the left endpoint of the T-window is determined by<sup>(2)</sup>

$$f_{\frac{1}{2}}^p(x) = x \tag{7}$$

$$D_x f_{\frac{1}{2}}^p(x) = 1 \tag{8}$$

where  $p = 3$  in this case.

For map (6), it is determined by the symbolic sequence  $\overline{RLR}$  or  $\overline{101}$ . In Fig. 1, the third iterate of map (6) is shown. The portion we are interested in a magnified in Fig. 2. As the parameter  $x_p$  increases, as long as the map remains in the window, the topological entropy will not change. The symbolic sequence of the largest  $x_p$  (i.e., the largest parameter that the map in Fig. 2 maps into itself) is  $\overline{RLLRLR}$ . This will define the right endpoint of the T-window represented by  $RL$  to be  $\overline{RLLRLR}$ .

Therefore for a T-window denoted by a superstable symbolic sequence

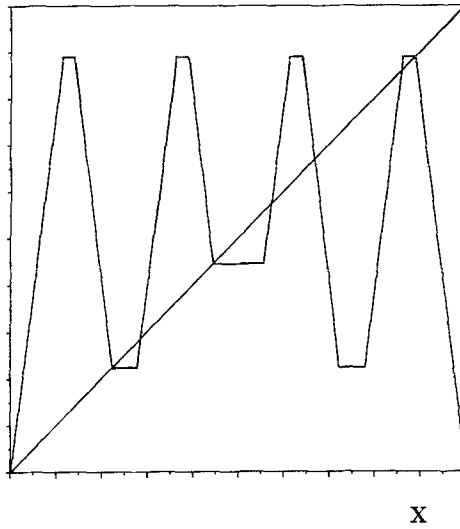


Fig. 1. The third iterate of map (6) at  $x_p = x_{100}$  showing the two fixed points  $x_{101}$  and  $x_{100}$ .

$P$ , the right endpoint is represented by  $PL\overline{P\overline{R}}$  if  $P$  is odd;  $PR\overline{P\overline{L}}$  otherwise. For maps (3)–(5), it is determined by the bisection method described in ref. 2. The left endpoints is determined by Eqs. (7) and (8) with  $p$  being the period of the superstable cycle represented by  $P$ . Details of the computation are given in ref. 2.

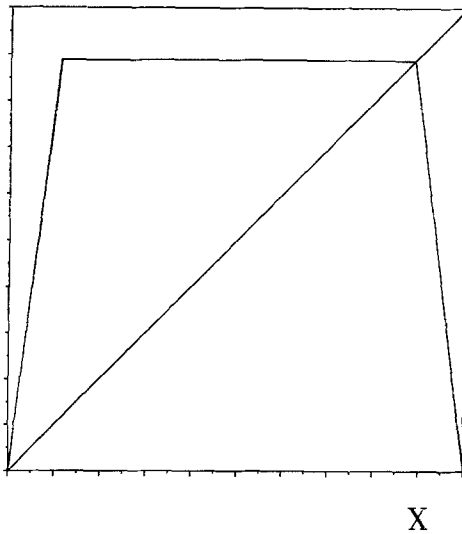


Fig. 2. The local dynamics of map (6) for  $x_p = x_{100}$ .

For map (6), given  $P = \overline{s_1 s_2 \cdots s_n}$ , where  $s_i = 1$  or  $0$ , the period points are given by

$$\begin{aligned}
 x_{\overline{s_1 s_2 \cdots s_n}} &= \frac{2^n}{2^n - 1} \cdot \varepsilon_1 \varepsilon_2 \cdots \varepsilon_n, & \sum_{k=1}^n s_k &= \text{even} \\
 &= \frac{2^{2n}}{2^{2n} - 1} \cdot \varepsilon_1 \varepsilon_2 \cdots \varepsilon_{2n}, & \sum_{k=1}^n s_k &= \text{odd}
 \end{aligned}
 \tag{9}$$

Therefore, for map (6), for a given superstable symbolic sequence  $P$ , the left endpoint is given by  $\overline{P1}$  if  $P$  is odd and  $\overline{P0}$  otherwise. The right endpoint is  $P0\overline{P1}$  if  $P$  is odd and  $P1\overline{P0}$  otherwise. Making use of (9), the corresponding endpoints in the parameter axis can be determined.

### 3. THE SCALING PROPERTIES OF T-WINDOWS

In the above, the windows of constant topological entropy or T-windows are constructed. An interesting question is, What is the measure of these windows and what universal behavior exists for this measure?

We will define a “fatness” exponent  $\beta$  introduced by Farmer<sup>(7)</sup> in studying the periodic windows.

Let  $T(\varepsilon)$  be the sum of the measures of all the windows with size greater than or equal to  $\varepsilon$ . Then  $T(0)$  is the measure of all the windows. It is conjectured that as  $\varepsilon \rightarrow 0$ ,

$$T(0) - T(\varepsilon) \simeq A\varepsilon^\beta \tag{10}$$

and the exponent  $\beta$  is universal for the class of maps with the same order of maximum, where  $A$  is a constant. Since

$$\log[T(0) - T(\varepsilon)] = \log A + \beta \log \varepsilon \tag{11}$$

$\beta$  can be determined from the curve of  $\log[T(0) - T(\varepsilon)]$  vs.  $\log \varepsilon$ .

We will arrange all these windows in the binary tree. Let  $S_n$  be the partial sum of all the windows in level  $\leq n$ . We also conjecture that for the class of maps with the same order of maximum,  $S_n \rightarrow S_\infty$  with the same asymptotic behavior:

$$S_n \simeq S_\infty e^{-\alpha/n^\kappa} \tag{12}$$

$$\log S_n \simeq \log S_\infty - \frac{\alpha}{n^\kappa} \tag{13}$$

That is,  $\kappa$  and  $\alpha$  is universal for maps with the same order of maximum.

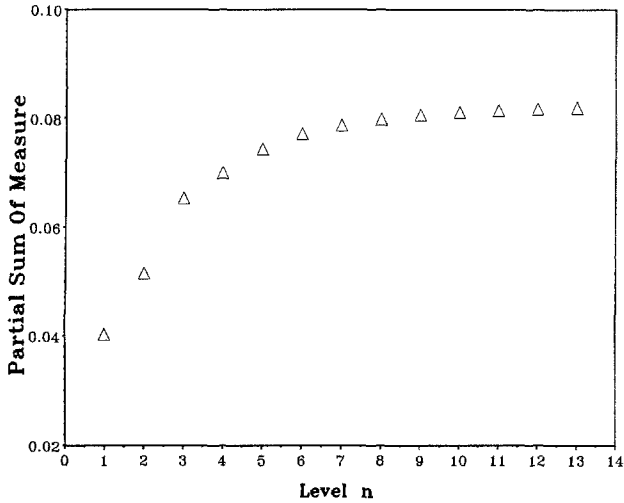


Fig. 3. The partial sum of the measure at level  $n$  plotted against  $n$  for map (3).

Up to 13 levels of the binary tree (more than 8000 windows) are included in our computation. The partial sum of the measures for maps (3) and (6) is plotted against level  $n$  in Figs. 3 and 4. As shown in the figure, for the quadratic maps, the convergence is very rapid. The convergence is much slower for map (6). For map (3), the fraction of the windows in the chaotic regime is  $0.1373 \pm 0.0005$ . For map (4), this number is

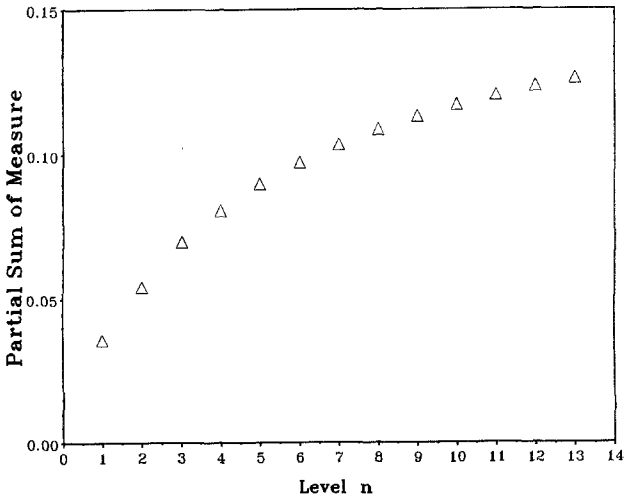


Fig. 4. The partial sum of the measure at level  $n$  plotted against  $n$  for map (6).

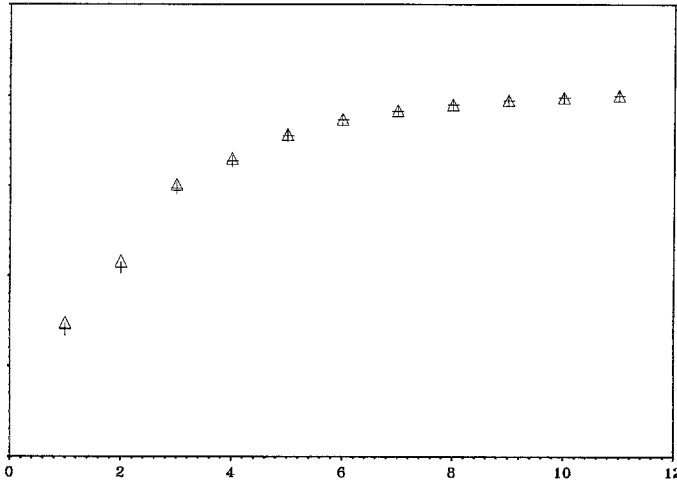


Fig. 5. The normalized partial sum of the measure at level  $n$  plotted against  $n$  for ( $\Delta$ ) map (3) and (+) map (4).

$0.1380 \pm 0.0007$ . It is  $0.1450 \pm 0.0003$  for map (5). To obtain these numbers the contributions of each of the 13 levels in the binary tree are studied and an extrapolation is made. The error is estimated to be greater than or equal to the difference between the extrapolated total measure and the measure obtained from the total 13 levels. It is hard to conclude whether this fraction is universal for quadratic maps. It is certainly different

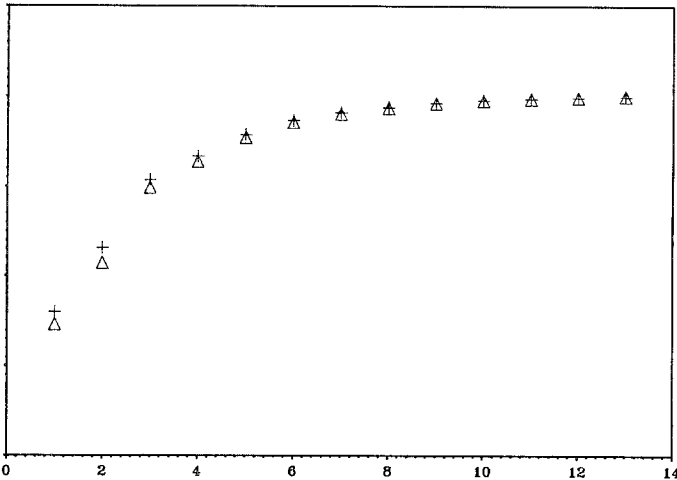


Fig. 6. The normalized partial sum of the measure at level  $n$  plotted against  $n$  for ( $\Delta$ ) map (3) and (+) (5).

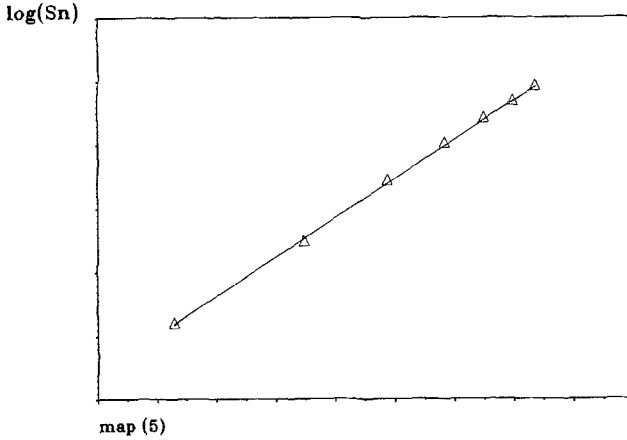


Fig. 7. Plot of  $\log S_n$  against  $-1/n^{2.5}$  for map (5) when  $n = 7, \dots, 13$ .

for map (3) and map (5), even though they have the same order of maximum.

The normalized partial sum of the measure  $S_n/S_{13}$  for maps (3) and (4) is shown in Fig. 5 [ $\Delta$ , map (3); +, map (4)]. The same is shown for map (3) and map (5) in Fig. 6. It is seen that the asymptotic behavior as  $n \rightarrow \infty$  is the same for maps (3)–(5), which supports our conjecture that  $S_n \rightarrow S_\infty$  with universal behavior for maps with the same order of maximum.

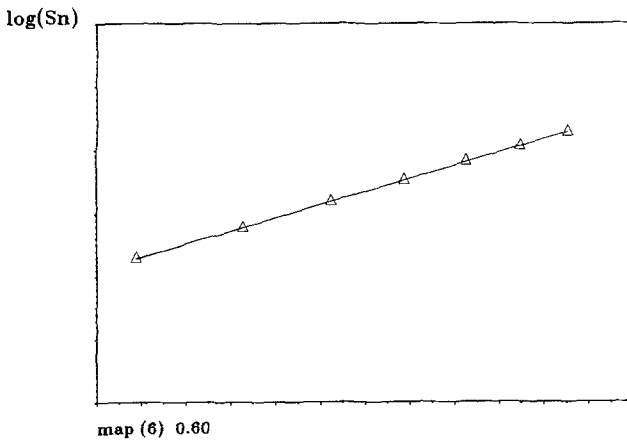


Fig. 8. Plot of  $\log S_n$  against  $-1/n^{0.6}$  for map (6) when  $n = 7, \dots, 13$ .



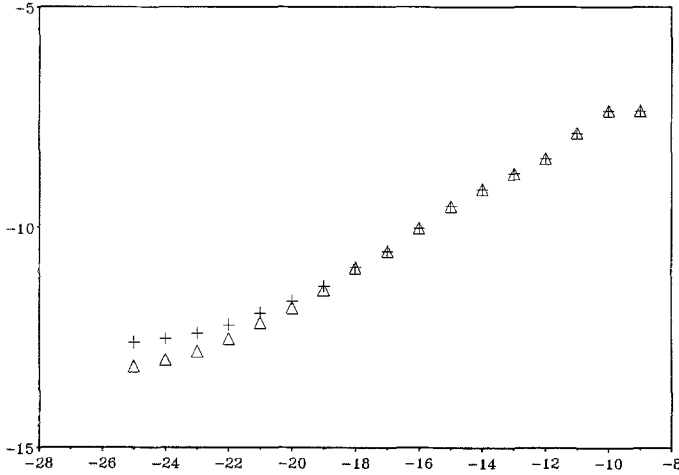


Fig. 9. Plot of  $\log_2 [T(0) - T(\epsilon)]$  against  $\log_2 \epsilon$  for map (4) ( $\triangle$ ,  $n = 13$ ; +,  $n = 12$ ).

We have found  $\kappa = 2.5 \pm 0.3$  and  $\alpha = 6.0 \pm 0.8$  for maps (3)–(5). We plot  $\log S_n$  against  $-1/n^{2.5}$  in Fig. 7 for  $n = 7, \dots, 13$ . For map (6),  $\kappa = 0.60 \pm 0.03$  and  $\alpha = 2.1 \pm 0.1$ . In Fig. 8,  $\log S_n$  is plotted against  $-1/n^{0.60}$  for  $n = 7, \dots, 13$ . Fitting  $\log S_n$  with a straight line for various exponents, we obtain  $\kappa$  as the best fit. The error of  $\kappa$  is the step size to the nearest fitting value. After  $\kappa$  is obtained,  $\alpha$  is estimated from the slope of the straight line.

In Figs. 9 and 10,  $\log_2 [T(0) - T(\epsilon)]$  is plotted against  $\log_2 \epsilon$  for maps

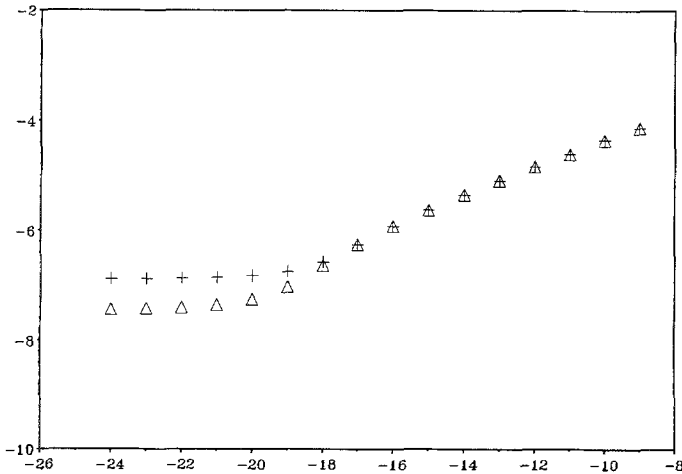


Fig. 10. Plot of  $[T(0) - T(\epsilon)]$  against  $\log_2 \epsilon$  for map (6) ( $\triangle$ ,  $n = 13$ ; +,  $n = 12$ ).

(3) and (6), where the estimated  $T(0)$  is used, and + signs represent the data including all the windows up to level 12 and  $\Delta$  represents the data of all the windows up to level 13. The deviation from a straight line indicates that some windows with size comparable to the deviation point are missed. For maps (3)–(5) the exponent  $\beta$  is estimated to be  $0.45 \pm 0.05$ , while for map (6),  $\beta = 0.30 \pm 0.05$ .

## ACKNOWLEDGMENTS

This research was conducted using the Cornell National Super-computer Facility, which receives major funding from the National Science Foundation and IBM Corporation.

I thank especially Predrag Cvitanovic, Paul Zweifel, and Mitchell Feigenbaum for valuable discussions. This work was supported by the National Science Foundation under grant no. DMS-8701050 and the U.S. Department of Energy under grant no. DE-FG05-87ER25033.

## REFERENCES

1. M. Metropolis, M. L. Stein, and P. R. Stein, *J. Combinatorial Theory (A)* **15**:25 (1973).
2. Y. Ge, E. Rusjan, and P. Zweifel, *J. Stat. Phys.* **59**:1265 (1990).
3. O. Biham and W. Wenzel, *Phys. Rev. Lett.* **63**:819 (1989).
4. R. Artuso, E. Aurell, and P. Cvitanovic, *Nonlinearity*, to appear.
5. R. Artuso, E. Aurell, and P. Cvitanovic, *Nonlinearity*, to appear.
6. P. Collet and J.-P. Eckmann, *Iterated Maps on the Interval as Dynamical Systems* (Birkhauser, Boston, 1980).
7. J. D. Farmer, *Phys. Rev. Lett.* **55**:351 (1985).